Proc. of the 30th International Slovak–Polish Scientific Conference on Machine Modelling and Simulations 2025

Experimental and Simulation Investigation of an Adaptive Pendulum-Tuned Mass Damper for Engineering Structures

K. Twardoch*, I. Kotłowski and K. Jaśkielewicz

Division of Numerical Methods and Intelligent Structures, Faculty of Automotive and Construction Machinery Engineering, Warsaw University of Technology, Ludwika Narbutta 84, 02-524 Warsaw, Poland

Doi: 10.12693/APhysPolA.149.S35 *e-mail: krzysztof.twardoch@pw.edu.pl

Slender civil structures remain vulnerable to dynamic actions, making robust, implementation-ready damping strategies a design priority. Building on our earlier feasibility study, which introduced an active, liquid-based pendulum-tuned mass damper with mass redistribution for real-time retuning in skyscrapers, the present work generalizes the concept to an adaptive pendulum-tuned mass damper in which variable pendulum length is the primary mechanism of adaptation — independent of any specific actuation technology. We developed a compact model of the coupled flexible frame–adaptive pendulum-tuned mass damper system with explicitly linearized descriptors suited for tuning and design. Then, we validated it experimentally on a shake-table using a flexible frame equipped with an adaptive pendulum-tuned mass damper. The quantitative comparison considers tuned and detuned settings under identical operating conditions. In numerical studies, adaptive length control at resonance achieves up to 85% suppression relative to a fixed-length tuned mass damper, confirming the performance margin available from geometric retuning. In shake-table experiments, the undamped reference shows a peak floor acceleration of 4.8 m/s^2. When optimally tuned (pendulum length 2 cm), the peak reduces to 1.8–2.0 m/s^2, i.e., by $\approx$ 60–63%. Detuned settings yield 3.7 m/s^2 (5 cm) and 3.2 m/s^2 (7 cm) at 5 Hz, corresponding to $\approx$ 23% and $\approx$ 33% reductions, respectively. These measured values, together with the model–experiment error analysis, substantiate the predictive accuracy of the proposed framework and quantify the sensitivity to mistuning. The novelty of this study lies in the generalization and experimental validation of an adaptive pendulum-tuned mass damper with variable pendulum length as a practical solution for vibration control in slender engineering structures. Unlike earlier feasibility studies focused on a specific liquid-based implementation, the proposed compact modeling framework and shake-table experiments confirm superior mitigation efficiency (up to 80–85% at resonance) and provide directly applicable design guidelines for real structures.

topics: tuned mass damper (TMD), adaptive pendulum-tuned mass damper (APTMD), vibration damping analysis, computational methods

1. Introduction

The relentless densification of contemporary urban cores has compelled architects and engineers to exploit the vertical dimension, resulting in a profusion of super-slender towers that deliver vast lettable floor area within exceedingly compact footprints. Yet, the very geometric efficiency that renders such structures desirable simultaneously amplifies their susceptibility to dynamic environmental actions, particularly along-wind and across-wind excitation. Excessive lateral accelerations also impair occupant comfort, most acutely on upper-story levels. Mitigating excessive lateral displacements and accelerations has therefore emerged as a cardinal design challenge. Prolonged exposure to environmental dynamic loads (primarily wind gusts and seismic ground motions) progressively undermines the structural integrity of super-tall buildings and, in extreme scenarios, may precipitate collapse. For these reasons, appropriate design solutions based on the use of tuned mass dampers (TMDs) for vibration control are employed.

Large-scale case studies underscore the TMD technological imperative, particularly the importance of vibration mitigation in tower buildings. Iconic super-tall buildings such as Burj Khalifa (828 m) in Dubai, Shanghai Tower (632 m), Taipei 101 (509.2 m) in Taiwan, the John Hancock Center (457.2 m with antenna masts) in Boston, and the Yokohama Landmark Tower (296.3 m), utilize pendulum-type TMDs weighing several hundred tons to reduce lateral accelerations during high-wind or seismic events. The Citigroup Center (278.9 m) in New York also integrates a mass

damper that mitigates serviceability-level sway, while the Millennium Bridge [1] in London utilizes a similar principle to suppress synchronous lateral excitation. Applications extend beyond civil engineering to include structural and mechanical engineering [2, 3].

A typical TMD consists of a secondary mass connected to the primary structure via a spring–damper pair. When the device is tuned to the natural frequency of the host system, energy is exchanged through destructive interference, diminishing motion amplitudes. The concept, formalized by Frahm [4] in 1909, was rigorously elaborated by Ormondroyd and Hartog [5, 6], as well as Brock [7], and has since been refined through optimization frameworks that account for mass ratio, damping level, and bandwidth. Fundamental studies of TMD theory and practice were provided in a book [8] and the extensive review article [9]. Subsequent scholarship has remained vigorous [10], reflecting the ongoing demand for design methodologies that optimize vibration-suppression performance across an expanding spectrum of practical applications.

TMDs are widely used in engineering, as demonstrated by studies [11–14]. Researchers are focusing on identifying the optimal parameters and corresponding TMD efficiency [15–18], as well as developing criteria for optimal tuning in damped structures [19]. Vibration-mitigation technologies can be broadly partitioned into passive and active categories [20, 21]. Passive devices (mainly TMDs) retain enduring appeal due to mechanical simplicity, fail-safe operation, and modest maintenance requirements [22]. However, their fixed mechanical properties impede real-time adaptability under time-varying excitation spectra [23, 24]. Active and semi-active solutions ameliorate this deficiency by modifying stiffness, damping, or mass properties in response to sensor feedback [25]. Despite superior adaptability, active schemes entail greater complexity, energy demand, and operational cost.

A significant increase in research on the dynamic behavior of civil infrastructure has been recorded over the past two decades [10, 13, 26, 27]. Vibrations induced by wind gusts, typhoons, and seismic ground motions compromise both serviceability and ultimate limit states of high-rise buildings and long-span bridges [16, 22, 24, 28, 29]. In response, contemporary practice increasingly adopts vibration control strategies (most prominently TMDs) to attenuate structural response and safeguard occupant comfort [11, 30, 31].

2. Research objective

Emerging research avenues extend beyond conventional mechanical TMD configurations, introducing fluid-mediated mass-modulation and adaptive pendulum structures [12, 32] that enhance tuning agility under multi-hazard loads [29]. These approaches target high-rise buildings, where dynamic characteristics may drift due to temperature variations, occupancy changes, or cumulative structural ageing.

Despite its success, the conventional pendulum TMD possesses a fixed cable length and, by extension, a fixed natural frequency. Consequently, its efficacy diminishes whenever the parent structure experiences modal drift due to operational or environmental variability. To address this limitation, an *adaptive pendulum-tuned mass damper* (APTMD) *with an adjustable-length cable* has been proposed, which is retuned via dynamic cable elongation. In practical applications, this may be caused by fluid-redistribution within the system, which adjusts cable length and changes its effective inertia and natural frequency on demand, thus adjusting the natural frequency while conferring adaptive capability. This mechanism enables real-time tuning in the vicinity of resonance to external excitations, significantly enhancing vibration-suppression performance compared to conventional fixed-tuning TMDs. This prevents resonance-inducing vibrations.

Multi-degree-of-freedom modeling and non-linear dynamic analyses expand the design space, enabling the creation of devices that retain efficacy under non-stationary, multi-hazard excitation. Our study follows this trend by investigating a variable-length pendulatory TMD capable of retuning to sustain near-optimal damping efficiency. This contribution delineates the conceptual framework, numerical modeling, and experimental validation of the APTMD-based system. A coupled absorber–structure model was formulated in the Lagrangian paradigm and implemented using the DynPy [33] programming library for Python, developed by the authors of articles [34–36] and in collaboration with their "Effective Python" Team. It is a specialized software development toolkit (models and algorithms) designed to perform advanced computations and dynamic simulations (for example [37, 38]) implemented in Python.

Complementary shake-table tests using a reduced-scale model of a building frame corroborate the predicted damping effectiveness and highlight the potential of this APTMD technology as a modernizable, low-energy solution for new-generation high-rise buildings. Simulated earthquakes at a reduced scale may help make buildings safer. Current research on a semi-adaptive vibration control system based on APTMD indicates that using a variable cable length as a tuning mechanism or a simplification for more complex models (elastic pendulum) yields interesting results with high convergence [39]. Therefore, further empirical and analytical studies of the variable-cable-length system are essential from a practical point of view and provide an important point of reference, despite the model simplifications applied.

The overarching purpose of our investigation is to quantify and specify the capacity of a pendulum-tuned mass damper (PTMD) to dampen serviceability-critical vibrations in high-rise buildings and other slender civil infrastructure exposed to dynamic hazards such as wind gusts, seismic ground motions, and anthropogenic excitation. Specifically, the study pursues three interrelated objectives:

(i) Establishing the baseline attenuation potential of a reference pendulum TMD by systematically varying canonical design variables under representative loading spectra.

(ii) Adaptive retuning via adjustable-length cable. Examination of a novel pendulum concept whose rope length $l(t)$ is adjustable in real time, thereby shifting its natural frequency to track time-varying structural modes. It is hypothesized that the system with an adaptive-length rope can outperform any static TMD configuration in terms of both peak reduction and robustness to modeling uncertainty. Through proper parameter selection (especially length), the pendulum's motion can be precisely controlled to maximize vibration damping and structural stability.

(iii) Validation of numerical simulations against shake-table experiments to confirm model accuracy and extract practical design guidelines. Minimizing the effects of maximum floor acceleration and total actuation energy in terms of lateral displacement of the parent structure (building frame), and thus improving the seismic safety of buildings.

By explaining the interdependencies among APTMD parameters, adaptive control rules, and structural responses, the research aims to provide experience-based recommendations that may enhance occupant comfort and safety in next-generation high-rise buildings that adhere to sustainable construction principles.

3. Methods and materials

3.1. Theoretical model and governing equations

The considered absorber prototype comprises a trolley–spring–damper assembly representing a single translational degree of freedom, to which a slender, axially flexible pendulum is hinged. Horizontal excitation is prescribed as a time-varying force $F_u = F(t)$ applied to the trolley. The damping action commences when the controlled cable extension mechanism is activated (for example, by sequentially pumping liquid into the pendulum tank), which shifts the pendulum's centre of gravity and activates the adaptive mass-tuning mechanism.

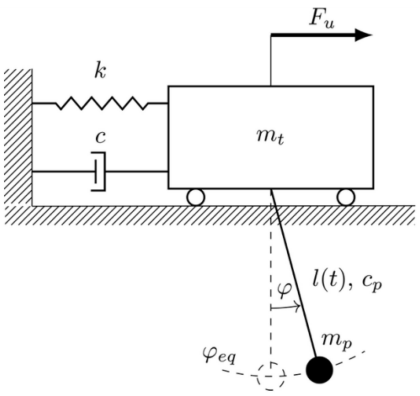

Fig. 1. The proposed APTMD-based system model.

A scheme of the adaptive pendulum-tuned mass damper (APTMD) under consideration is shown in Fig. 1.

It is worth noting that in Fig. 1, c denotes the damping of the primary structure, while c_p denotes the viscous damping associated with the motion of the pendulum mass relative to the main structure. The coefficient c_p represents an equivalent linear viscous damping of the pendulum subsystem. The coefficient c_p is introduced into the equations of motion as a small viscous damping that accounts for hinge friction and minor mechanical losses in the relative motion between the pendulum and the main structure. Its inclusion has two reasons. First, it reflects the presence of inherent dissipation in the experimental pendulum mechanism. Second, it ensures the numerical solution's stability and prevents non-physical amplification near the tuned condition, which is known to occur in idealized undamped absorber models.

To avoid any artificial influence on the system's dynamic characteristics, c_p was chosen to avoid significantly altering the natural frequencies or the APTMD tuning. In all numerical simulations, the pendulum damping coefficient was set to $c_p = c$. This choice provides sufficient damping to stabilize the numerical integration of the coupled system and is consistent with the expected small inherent dissipation of the experimental pendulum. The performed sensitivity check confirmed that this assumption does not lead to noticeable changes in the natural frequencies or in the APTMD tuning. The adopted value of c_p does not bias the assessment of the vibration reduction achieved by the proposed APTMD configuration. The effect of c_p is limited to a slight increase in the decay rate of transient vibrations, while the resonance frequencies, tuning condition, and comparative performance of tuned, untuned, and inactive configurations remain practically unchanged. Therefore, c_p is not treated as an additional design parameter, but as a numerically and physically justified assumption that regularizes the model.

TABLE I

APTMD-based system parameters selected for simulation investigation.

Parameter	Unit	Value
m_t	kg	0.7
m_p	kg	0.1
c	$\frac{\mathrm{N\ s}}{m}$	10
c_p	$\frac{\mathrm{N\ s}}{m}$	10
k	$\frac{\mathrm{N}}{m}$	80
l	m	0.02 / 0.05 / 0.075

The system dynamics are formulated within the framework of Lagrangian mechanics. Generalized coordinates are defined for the cart translation, pendulum rotation, and cable elongation, and the Euler–Lagrange equations are subsequently applied to obtain the governing equations of motion in compact matrix form. This procedure establishes a mathematically rigorous representation of the proposed APTMD-based system. The vibration parameters for this system's physical model are summarized in Table I. The equations of motion derived using the Lagrangian formulation in general form are expressed as follows

$$L = E_k - E_p, \tag{1}$$

where E_k is the system kinetic energy, and E_p is the system potential energy.

The system Lagrangian has the following form

$$L = g\, m_p\, l\, \cos(\varphi) - \frac{1}{2}\, k x^2 + \frac{1}{2}\, m_p\, l^2\, \dot{\varphi}^2 + m_p\, l\, \cos(\varphi)\dot{\varphi}\, \dot{x} + \frac{1}{2}\, m_p \dot{x}^2 + \frac{1}{2}\, m_t \dot{x}^2. \tag{2}$$

The general form of the equations of motion is as follows

$$-F\sin(\Omega t) + c\dot{x} + kx - m_p l \sin(\varphi)\dot{\varphi}^2 + m_p l \cos(\varphi)\ddot{\varphi} + m_p \cos(\varphi)\, \dot{\varphi}\, \dot{l} + m_p \ddot{x} + m_t\, \ddot{x} = 0, \tag{3}$$

$$c_p\dot{\varphi} + g m_p l \sin(\varphi) + m_p l^2 \sin^2(\varphi)\ddot{\varphi} + m_p l^2 \cos^2(\varphi)\ddot{\varphi} + 2 m_p l \sin^2(\varphi)\dot{\varphi}\, \dot{l} + 2 m_p l \cos^2(\varphi)\dot{\varphi}\, \dot{l} + m_p l \cos(\varphi)\, \ddot{x} + m_p \cos(\varphi)\, \dot{l}\, \dot{x} = 0. \tag{4}$$

To facilitate analytical and numerical treatment, the nonlinear model (see (3)–(4)) was linearized around the equilibrium position $\varphi_{eq} = 0$: $\sin(\varphi) \approx \varphi \wedge \cos(\varphi) \approx 1 \Rightarrow \sin(\varphi) = \varphi \wedge \cos(\varphi) = 1$. Higher-order coupling terms were neglected. The complexity of the nonlinear, coupled system of differential equations that comprehensively describes the dynamics of the studied object makes it impossible to obtain an analytical solution in a general form. To get a tractable representation for control synthesis and efficient numerical simulation, the system is linearized under small-perturbation assumptions about a selected equilibrium configuration (operating point). The linearized state-space model, valid in the neighborhood of this operating point, is as follows

$$-F\sin(\Omega t) + c\,\dot{x} + kx + m_p l\,\ddot{\varphi} + m_p\,\dot{\varphi}\,\dot{l} + \big(m_p + m_t\big)\,\ddot{x} = 0, \tag{5}$$

$$c_p\dot{\varphi} + g m_p l\,\varphi + m_p l^2\,\ddot{\varphi} + 2 m_p l\,\dot{\varphi}\,\dot{l} + m_p l\,\ddot{x} + m_p\,\dot{l}\,\dot{x} = 0. \tag{6}$$

The linearized model, expressed by (5)–(6), allows for an efficient evaluation of system dynamics near the equilibrium state. Inspection of the state-space structure reveals partial coupling; thus, (5) and (6) constitute a coupled system that must be solved concurrently.

This decomposition streamlines both analytical and computational treatment. With a linear model, closed-form solutions can be obtained analytically, enabling rigorous interpretation of the system's dynamic characteristics and systematic parametric studies under varied excitation conditions.

External forcing is applied exclusively to the primary structure in the form of the harmonic excitation defined by

$$F_u = -F\sin(\Omega t), \tag{7}$$

with no direct actuation on the absorber.

Further analytical calculations performed on linearized equations provide a canonical matrix representation of the APTMD-based system model. The inertia matrix M,

$$M = \begin{bmatrix} m_p + m_t & m_p\, l \\ m_p\, l & m_p\, l^2 \end{bmatrix}, \tag{8}$$

represents inertial coupling among the generalized coordinates associated with each degree of freedom. The stiffness matrix K,

$$K = \begin{bmatrix} k & 0 \\ 0 & g\, m_p\, l \end{bmatrix}, \tag{9}$$

relates forces acting on a system to its displacements. The damping matrix C,

$$C = \begin{bmatrix} c & m_p\,\dot{l} \\ m_p\,\dot{l} & c_p + 2 m_p\, l\,\dot{l} \end{bmatrix}, \tag{10}$$

characterizes energy dissipation in the system, thereby governing the damping of vibration amplitudes (essentially S models how vibrations diminish over time). The variable notation used in (8)–(10) is: time t, pendulum damping coefficient c_p, damping coefficient c, instantaneous cable length l, cable length change rate $\dot{l}$, and pendulum lumped mass m_p.

The presented model is non-linear, coupled, and non-autonomous. Due to its complexity and nonlinear nature, it is not possible to obtain accurate analytical solutions. This is the main reason for linearizing the system around a selected operating

point. Further numerical integration enables the calculation of the dynamic response of the investigated concept.

The formulated model is non-linear, coupled, and non-autonomous, rendering closed-form analytical solutions intractable. Consequently, the system is linearized about a selected equilibrium state, and numerical time integration is subsequently applied to compute the dynamic response of the proposed absorber configuration, i.e., APTMD. The results of numerical analyses using this mathematical model are presented in Sect. 4.1, which discusses the simulation and experimental investigations.

3.2. Test stand

Experimental validation is necessary to verify the reliability of simulation results. This is a fundamental issue in investigations based on modeling and computer simulation. Therefore, a test stand was designed and assembled to empirically evaluate the proposed concept, as shown in Fig. 2. It is a stable structure as a supporting frame, ensuring suitable working conditions and safety. All stand components are assembled on it. This test stand's principle is based on the oscillatory motion. The tested APTMD-based mechanism is placed in a movable reference model of the building frame mounted on a shake-table [5]. This frame was modeled on a reduced scale as a flexible frame [3], and a weight [4] is installed on it using an adjustable-length cable savers as the adaptive pendulum-tuned mass damper (APTMD) device. The shake-table [5] is a special trolley (carriage) that moves along guide rails. An electric motor [1] with a belt drive [2] powers the shake-table [5] in a reciprocating motion via a connecting rod [6]. The table shaking velocity depends on the motor speed, which is regulated by an inverter [8]. This way, the frequency of the applied force is adjusted.

When the test stand is operating, vibrations are generated and transmitted from the shake-table to the flexible frame. These vibrations cause oscillations of a pendulum with its weight (APTMD) inside the flexible frame. A measurement system consisting of two accelerometers [7], a data acquisition device (NI cDAQ-9174), and a measurement card (NI-9230) is used to measure vibrations.

The tested system with APTMD was designed to allow control of damper inertia by adjusting either the pendulum mass or the cable length. Lengthening or shortening the pendulum cable affects the resonance frequencies of this system. Furthermore, analysis of the investigated system and the governing equations obtained allows us to state that the system's dynamics can also be assessed by performing a sequence of quasi-static tests.

It was assumed that a damped object is a sprung mass with a single degree of freedom (SDOF).

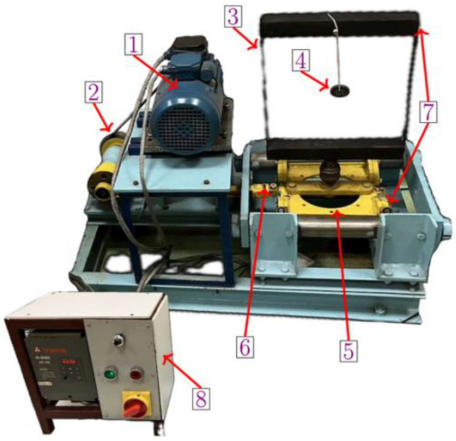

Fig. 2. Test stand for APTMD on a shake-table using a reduced-scale building frame model (flexible frame) [39].

Moreover, a lack of additional external damping was adopted to make the analysis as long as possible, and the adjustable-length cable of the adaptive damper can be tuned in dynamic or static mode. To extend the scope of tests, excitation should be applied kinematically or impulsively during the empirical investigation.

4. Results and discussions

4.1. Simulation results

Mathematical model analysis enables the determination of the system's dynamic behavior depending on changes in its parameters. Previous studies have shown that the parameters of a damped system can be estimated by performing simple static experiments [39]. It turns out that the activation time of the proposed pendulum damper solution is the most crucial parameter and must be evaluated. This approach facilitates a deeper understanding of the suppression mechanisms and enables empirical testing.

Figure 3 presents the numerical tests for four activation times. Simulations for $t_0 = 0$ s and $t_0 = 90$ s as reference cases that represent a system with a passive tuned absorber ($t_0 = 0$ s) and a system without an absorber ($t_0 = 90$ s). The simulation parameters were chosen so that the system was in a resonant state before the damper was activated. After the damper was activated, it was immediately tuned to eliminate the resonance.

Spectral analysis of the system response (Fig. 4) for different activation times t_0 provides further insight into the operating mechanism of the APTMD. For $t_0 = 90$ s, when the damper remains practically inactive during the considered interval, the spectrum exhibits a single dominant peak. This peak corresponds to the excitation frequency, chosen

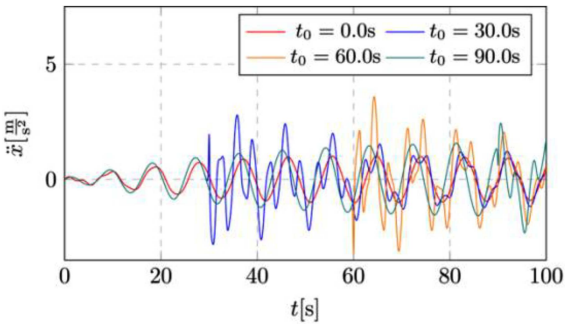

Fig. 3. Trolley vibration accelerations for various damping activation times.

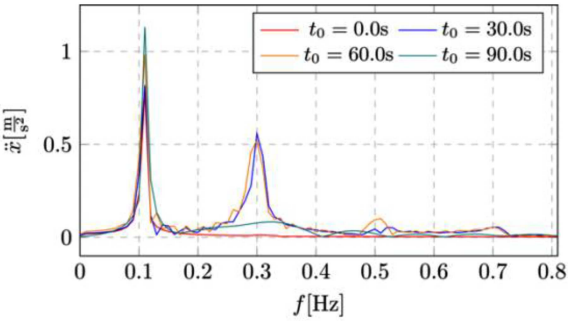

Fig. 4. Frequency spectra of trolley vibration accelerations for various damping activation times, t_0.

close to the fundamental natural frequency of the trolley–structure system without the APTMD, and thus represents the resonance of the uncontrolled system. The spectrum shows a single component at the undamped system's resonance frequency, as assumed.

When the APTMD is activated ($t_0 = 0$, 30, 60 s), this single resonance peak splits into two distinct components with significantly lower amplitudes. The lower-frequency component is associated with the excitation of the coupled trolley–APTMD system, in which the motion of the primary structure is dominant. The higher-frequency component corresponds to one of the eigenvalues and reflects the energy transfer from the trolley to the absorber. Observed splitting effect of a resonance confirms that the APTMD effectively modifies the system's dynamic characteristics.

A comparison of the spectra shows that decreasing the activation delay leads to a systematic reduction in the overall vibration level. The lowest amplitudes are obtained for $t_0 = 0$ s, i.e., when the damper is active and tuned from the onset of resonance excitation. This confirms that both the presence of the APTMD and the appropriate choice of activation time are crucial for preventing excessive resonant vibrations.

The research conducted allows us to conclude that the activation time plays a key role in the vibration suppression process. It is clear to see that

TABLE II

Experimental setup parameters used in vibration tests of the APTMD-based system.

Parameter	Unit	Value
m_t	kg	0.7
m_p	kg	0.1
c	$\frac{\text{N s}}{\text{m}}$	10
c_p	$\frac{\text{N s}}{\text{m}}$	10
k	$\frac{\text{N}}{\text{m}}$	80
l	m	0.02 / 0.05 / 0.075
Excitation range	Hz	2–10
DAQ model		NI 9230+NI cDAQ-9174
Measurement time	s	100

vibrations of the system increase in the case of a system without an activated damper (activation time is 90 s). Longer analyses show that the system without APTMD operates in the resonance zone. Proper selection of the activation time prevents an unbounded increase in vibration levels. The trolley's lowest vibration level occurs when the activation time is zero, meaning the damper was activated at the moment of resonance excitation. It can be concluded that as the activation delay reduces, the total vibration level decreases.

4.2. Test stand results

The experimental research consisted of two parts: a preparatory phase and empirical testing. At the beginning (during the preparatory phase), resonance frequency calculations were performed for the object with and without a pendulum. The model was then mounted in a forcing machine — on the shake-table of the test stand equipped with an inverter, whose frequency can be smoothly adjusted in the range from 4 to 20 Hz. A belt drive with a 1:2 transmission ratio was used on the test stand, allowing excitation frequency in the range from 2 to 10 Hz. The adjustment was made using a knob. Measurements were initiated at the resonance frequency to verify the accuracy of the theoretical calculations, and the calculations were then adjusted accordingly. Accelerations were measured using an acceleration sensor, one mounted on a movable base and the other on the damped object. Before starting the acceleration measurements, the empirically verified resonance frequency was set as the starting point.

Then, the empirical research stage began. The first case study was a system with TMD disabled. This configuration served as a reference case when the pendulum functioned solely as an inertial element. With minimal length and no added mass, the pendulum was dynamically decoupled

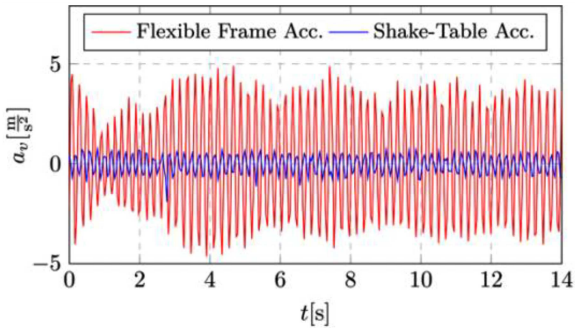

Fig. 5. Structure vibration acceleration with the pendulum turned off (APTMD inactive).

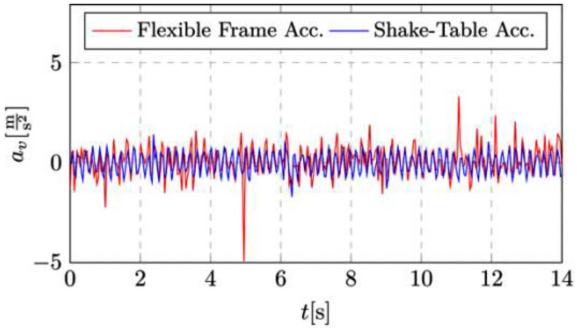

Fig. 6. Structure vibration acceleration for the pendulum with a length of 2 cm.

(isolated) from the movement of the building frame model (flexible frame). Analysis of time-series data showed that the structure experienced distinct periodic vibrations characterized by large acceleration amplitudes. The pendulum's motion was weak, delayed, and showed little correlation with the building's movement, indicating minimal energy exchange between the two systems. From a vibration-damping perspective, this confirmed that without sufficient mass or proper tuning, the pendulum does not function as an effective damping mechanism. Instead, it behaves as a passive element that neither absorbs nor dissipates energy, thus failing to reduce structural vibrations.

The test stand parameters used in the experiments are shown in Table II (see Sect. 3.2 for additional details).

To ensure consistency with the test stand nomenclature, the time series names in the legends are as follows. Shake-table acceleration refers to the horizontal kinematic excitation expressed as the table vibration acceleration. In turn, the system response in the form of the acceleration of the building frame model is referred to as flexible frame acceleration.

The results for the reference case are shown in Fig. 5. In the case without the pendulum, the acceleration profiles of the skyscraper were 4.8 m/s^2.

In the next case, an absorber with a length of 2 cm (Fig. 6) was considered. In this case, the pendulum's mass and length were adjusted to closely align its natural frequency with the dominant natural frequency of the structure. This adjustment resulted in the characteristic behavior of a tuned mass damper system, with the pendulum oscillating in anti-phase with the building's motion. Such dynamics enabled the pendulum to effectively absorb kinetic energy from the primary structure. Figure 6 shows an apparent decrease in the peak acceleration amplitudes of the building frame, indicating improved damping efficiency.

The accelerations of the building frame decreased to $\approx$ 1.8–2 m/s^2. The anti-phase oscillation generated a counterforce that diminished the building

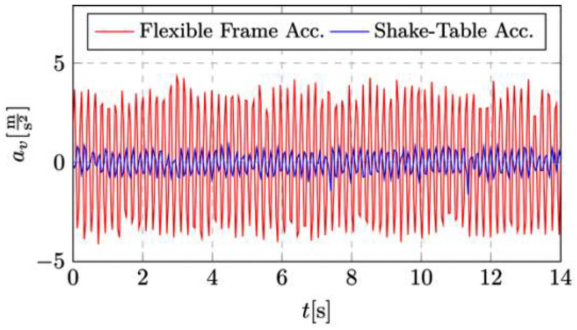

Fig. 7. Structure vibration acceleration for the pendulum with a length of 5 cm.

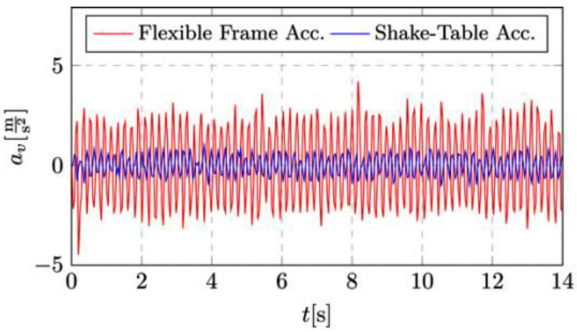

Fig. 8. Structure vibration acceleration for the pendulum with a length of 7 cm.

frame sway and vibration intensity. This outcome reflects practical applications, such as the massive pendulum installed in Taipei 101, which reduces structural sway during seismic events and typhoons. The results confirmed that precise tuning is crucial for a secondary oscillator to significantly reduce undesirable vibrations.

Next, two further cases were analyzed, using pendulums with lengths of 5 cm (Fig. 7) and 7 cm (Fig. 8). When the pendulum was lengthened to 5 cm or 7 cm, its natural frequency shifted away from the excitation frequency of the structure. Although the pendulum remained responsive to base

motions, the energy transfer between the pendulum and the building was less effective. The acceleration amplitudes of the structure increased compared to the optimally tuned case (Fig. 6), as indicated by higher peaks in the measured data. For a pendulum length of 5 cm (Fig. 7) and a forcing of 5 Hz, the accelerations were 3.7 m/s^2. For a pendulum length of 7 cm (Fig. 8) and a forcing of 5 Hz, the accelerations were 3.2 m/s^2.

Less-accurate tuning sometimes led to amplification of specific vibration harmonics due to unfavorable phase relationships between the two systems. Such behavior highlights the sensitivity of tuned mass dampers to parameter variations, where even minor detuning can significantly impair vibration reduction performance. While this configuration still outperformed the baseline "no weight" scenario, it underscored the critical importance of accurate tuning for effective vibration mitigation.

As shown, the best result was achieved with the pendulum length of 2 cm. The acceleration of the damped object (flexible frame) was reduced by a factor of 5. The amplitudes of the vibrations outside the tuning range depend directly on the pendulum length, allowing smooth control of the dynamic response of the damped object.

Relative errors were computed for each measurement series. The application of the relative error metric enables a quantification of result accuracy in proportion to the magnitude of the measured variables. This provides a dimensionless measure of deviation that remains consistent regardless of amplitude variations.

The calculated relative errors ranged from $\approx 0.6\%$ to 2.6%. Representative values recorded at successive temporal intervals were 0.92%, 1.73%, 2.59%, 1.44%, and 0.59%.

To increase reliability, gross errors in the acceleration signals were removed using a rolling-median-based filtering procedure. After eliminating such spurious peaks, the physically meaningful acceleration range for the reference measurement was found to lie between -0.866 and 0.687 m/s^2. This confirms that the experimental signals remain well within expected dynamic limits and exhibit no irregular behavior once noise artefacts are suppressed.

By normalizing measurement discrepancies relative to their corresponding signal magnitudes, the relative error provides a more robust and insightful representation of measurement precision across different vibration amplitudes. This methodological choice facilitates an objective evaluation of the congruence between experimental results and theoretical predictions, independent of the absolute acceleration levels.

It should be highlighted that all tests show vibration levels and spectral structures consistent with those observed in the simulations. This proves that the presented model accurately reflects the analyzed phenomenon and confirms the validity of the applied assumptions.

4.3. Result discussion

The dynamic behavior and vibration-mitigation capabilities of the APTMD-based system, which consists of a pendulum-tuned damper with a weight on an adjustable-length cable mounted inside the flexible frame, serving as the building structure model, were investigated. Such a complex structural model was subjected to periodic excitations. The adjustable pendulum parameters (mass and length) allow tuning its natural frequency relative to the main structure's natural frequency. Four configurations were analyzed, each showing different tuning accuracy and its consequent effect on the structure's vibration response.

When the pendulum has a minimum length and no additional mass (weight), it acts as an inertial accessory, which causes dynamic decoupling (isolation) from the building structure movement. Time-series data reveal that the structure experiences significant periodic vibrations with large acceleration amplitudes. The pendulum's response is weak, delayed, and largely uncorrelated with the building's movement. This indicates negligible energy exchange between the main structure and the pendulum. In terms of vibration control, this confirms that without adequate mass and proper length tuning, the pendulum does not function as an effective damping device. It behaves as a passive element that neither absorbs nor dissipates energy, providing no vibration mitigation for the structure.

A special case for the complex structure of the proposed APTMD-based system is the variant with a pendulum length of 2 cm. Precise adjustment of the length to weight allows the pendulum's natural frequency to be accurately matched with the dominant natural frequency of the building structure. In this arrangement, the system exhibits the characteristic behavior of a tuned mass damper. Indeed, the pendulum oscillates in anti-phase with the building's structural movement, effectively absorbing kinetic energy from the central system. The experimental results (on the test stand) indicate a significant reduction in the peak acceleration amplitudes of the tested structure, which means improved damping effectiveness. The counter-phase oscillations result in a counteracting force that reduces the structure's sway and the vibration intensity. It can be considered the optimal tuning variant.

Further research has shown that when the pendulum length is increased to 5 cm or 7 cm, its natural frequency deviates from the building's excitation frequency. Although the pendulum remains active and responds to base structure movement, the vibration energy transfer between the two systems is no longer optimal. The building accelerations increase relative to the optimally tuned pendulum with a length of 2 cm, as indicated by higher peak accelerations in the acceleration data. This suboptimal tuning can amplify specific vibration

harmonics due to unfavorable phase relationships between the building and the pendulum. This behavior highlights the sensitivity of TMD systems to parameter changes. Even a slight detuning causes a noticeable deterioration in vibration-damping performance. Although this configuration still outperforms the "no weight" case, it clearly shows the critical importance of accurate tuning in TMD applications. This can be useful for vibration-level control, e.g., from an energy-harvesting perspective.

Analysis of the results of the simulations and tests performed allows us to observe that:

- The variable cable length of the model corresponds with empirical experiments conducted for selected linkage lengths.
- Minor discrepancies in the absorber's activation or deactivation from reference cases do not significantly affect the spectral structure and overall vibration level of the damped object.

This indicates that the methodology used has proven effective in practice, and the dynamic length adjustment process can be omitted when selecting absorber parameters and planning control strategies.

5. Conclusions

It can be concluded that the possibility of controlling vibration level by APTMD has been proven in both theoretical and empirical ways. As part of the work, a method for tuning PTMD within the planned excitation range was developed. Both analytical and physical models were upgraded to increase accuracy, provide a better understanding of the conducted research, and prove that the created mathematical model is accurate and allows for predicting the behavior of a life-scale model. Based on the investigation results, the following insights were stated:

- The vibration acceleration for tuned APTMD (with an optimal pendulum length of 2 cm) is approximately 3 times lower than for the system without this damping device (pendulum disabled/locked).
- The vibration acceleration for untuned APTMD (with a pendulum length of 7 cm) is comparable to the system with the pendulum turned off (inactive APTMD) — their values represent approximately 80% of vibration acceleration without APTMD.
- The undetermined state lasts approximately 0.5 s, which enables effective use of the solution under continuous load conditions.
- The range of 3-7 cm is a significant area where it is possible to control the vibration level, for example, for energy harvesting.

By an undetermined state, we mean a transient dynamic state of the system that occurs after activation or retuning of the APTMD system, before a steady state is achieved. For the undetermined (transient) state the value of ≈ 0.5 s was obtained from the measured acceleration time histories after APTMD activation by identifying the time required for the main structure's response to reach a stable, steady-state regime. For all investigated configurations, this transient did not exceed ≈ 0.5 s. This value was determined directly from Fig. 8 (for a pendulum length of 7 cm — the most unfavorable case), where the transient time is most clearly visible. In this graph, the time from activation to response stabilization is ≈ 0.4–0.5 s. The value of 0.5 s is thus adopted as a conservative characteristic time. It reflects the intrinsic properties of the damped-coupled system rather than a specific feature of the APTMD itself. This short transient confirms that the proposed solution can be effectively used under continuous-load conditions.

Compared with classical fixed-tuning TMDs, the proposed APTMD yields a new understanding of adaptive damping behavior and delivers actionable guidance for design. First, adaptation via variable pendulum length $l(t)$ preserves near-optimal tuning as structural/excitation frequencies drift, maintaining the favorable resonance-splitting regime that suppresses peaks (whereas late/inactive cases revert to the single uncontrolled resonance). Second, the adaptive action is operationally practical — the post-retuning transient is short (≈ 0.5 s), enabling updates during continuous operation. Third, experiments quantify robustness — the optimally tuned setting lowers peak acceleration from 4.8 m/s^2 to 1.8–2.0 m/s^2 (≈ 60–63%), while detuned settings still achieve ≈ 23–33% reduction; simulations indicate up to 80–85% suppression at resonance, revealing the performance margin recoverable by retuning. Finally, setting $c_p = c$ stabilizes the coupled dynamics without shifting eigenfrequencies, so control synthesis can focus on $l(t)$ as the principal adaptive variable. Collectively, these results establish APTMDs as implementation-ready devices that: (i) augment mitigation beyond classical TMDs at resonance, (ii) sustain effectiveness under modal drift, and (iii) admit simple supervisory policies (i.e., "activate at or before resonance and retune $l(t)$ to maintain the split") for real structures.

Although the experiment successfully demonstrated the fundamental principles of a tuned mass damper (TMD) system, several aspects could be improved to enhance the accuracy, reliability, and applicability of the results. The experimental setup would benefit from a more precise method of tuning the pendulum parameters. Introducing adjustable mass elements or a mechanism allowing finer control over the pendulum length would enable more accurate resonance matching and a broader investigation of tuning sensitivity. Another area for enhancement involves the range and types of excitations

applied. Rather than employing only periodic sinusoidal inputs, incorporating random or seismic-like excitations would better simulate real-world conditions and allow assessment of the TMD's effectiveness under more complex loading scenarios.

References

[1] T. Fitzpatrick, P. Dallard, S. Le Bourva, A. Low, R.R. Smith, M. Willford, *Linking London: The Millennium Bridge*, Royal Academy of Engineering, 2001.

[2] G. Stefko, "Structural Mechanics and Dynamics Branch", NTRS — NASA Technical Reports Server, 2003.

[3] B. Xu, Ch. Xiang, Y. Qin, P. Ding, M. Dong, *IEEE Access* **6**, 60274 (2018).

[4] H. Frahm, Device for damping vibrations of bodies, US Patent US989958A, 1911.

[5] J. Ormondroyd, J.P. Den Hartog, *Trans. Ame. Soc. Mech. Eng.* **49–50**, 021007 (1928).

[6] J.P. Den Hartog, *Mechanical Vibrations*, Dover Publications, 1985.

[7] I.E. Brock, *J. Appl. Mech* **13**, A284 (1946).

[8] B.G. Korenev, L. Reznikov, *Dynamic Vibration Absorbers: Theory and Technical Applications*, Nauka, Moscow 1988.

[9] J.Q. Sun, M.R. Jolly, M.A. Norris, *J. Mech. Des.* **117**, 234 (1995).

[10] F. Yang, R. Sedaghati, E. Esmailzadeh, *J. Vib. Control* **28**, 812 (2021).

[11] S. Elias, V. Matsagar, *Ann. Rev. Control* **44**, 129 (2017).

[12] Y.-A. Lai, C.S.W. Yang, K.-H. Lien, L.-L. Chung, L.-Y. Wu, *Struct. Control Health Monit.* **23**, 1218 (2016).

[13] P.Y. Lin, L.L. Chung, C.H. Loh, *Comput.-Aided Civil Infrastruct. Eng.* **20**, 35 (2005).

[14] M. Żurawski, R. Zalewski, B. Chiliński, *J. Theor. Appl. Mech.* **58**, 811 (2020).

[15] S.V. Bakre, R.S. Jangid, *Struct. Control Health Monit.* **14**, 448 (2007).

[16] R.R. Gerges, B.J. Vickery, *Struct. Des. Tall Spec. Build.* **14**, 353 (2005).

[17] D. Pietrosanti, M. De Angelis, M. Basili, *Earthq. Eng. Struct. Dyn.* **46**, 1367 (2017).

[18] G. Bertollucci Colherinhas, F. Petrini, M.V.G. de Morais, F. Bontempi, *Wind Energy* **24**, 573 (2021).

[19] A. Ghosh, B. Basu, *Struct. Control Health Monit.* **14**, 681 (2007).

[20] E. Diez-Jimenez, R. Rizzo, M.-J. Gómez-García, E. Corral-Abad, *Shock Vib.* **2019**, 1250707 (2019).

[21] H. Gao, C. Wang, Ch. Huang, W. Shi, L. Huo, *Shock Vib.* **2020**, 9605028 (2020).

[22] M. Gutierrez Soto, H. Adeli, *Eng. Struct.* **186**, 536 (2019).

[23] I. Febrin Anas, T. Jafril, A. Syah Bintang, *MATEC Web Conf.* **229**, 01013 (2018).

[24] S. Elias, V. Matsagar, *J. Build. Eng.* **15**, 51 (2018).

[25] L. Gagnon, M. Morandini, G.L. Ghiringhelli, *J. Sound Vib.* **459**, 114865 (2019).

[26] R. Lewandowski, *Redukcja Drgań Konstrukcji Budowlanych*, Wyd. Nauk. PWN, Warsaw 2014 (in Polish).

[27] Z. Lu, Z. Wang, S.F. Masri, X. Lu, *Struct. Control Health Monit.* **25**, e2058 (2018).

[28] E.D. Khiabani, H. Ghaffarzadeh, B. Shiri, J. Katebi, *J. Vib. Control* **26**, 1445 (2020).

[29] D. Demetriou, N. Nikitas, *Appl. Sci.* **6**, 397 (2016).

[30] J. Alves Guimaraes, M. dos Reis Farias, M.T.B. César, R.M.M. Carneiro de Barros, *Rev. Eng. Pesqui. Apl.* **6**, 55 (2021).

[31] T. Pais, D. Boote, *Ocean Eng.* **141**, 249 (2017).

[32] L. Wang, W. Shi, Y. Zhou, *Struct. Des. Tall Spec. Build.* **28**, e1561 (2019).

[33] B. Chiliński, DynPy, GitHub, 2025.

[34] A. Mackojć, B. Chiliński, *Bull. Pol. Acad. Sci. Tech. Sci.* **70**, e139003 (2022).

[35] B. Chiliński, A. Mackojć, K. Mackojć, *Ocean Eng.* **259**, 111835 (2022).

[36] K. Twardoch, D. Sierociński, *Sustainability* **17**, 1837 (2025).

[37] D. Sierociński, B. Chiliński, F. Gawiński, A. Radomski, P. Przybyłowicz, *Energies* **18**, 332 (2025).

[38] B. Chiliński, R. Kwiatkowski, K. Twardoch, A. Mackojć, *Bull. Pol. Acad. Sci. Tech. Sci.* **73**, e154285 (2025).

[39] K. Twardoch, K. Górski, R. Kwiatkowski, K. Jaśkielewicz, B. Chiliński, *Sustainability* **17**, 6301 (2025).